Wood-Derived Porous Ceramics *via* Infiltration of SiO$_2$-Sol and Carbothermal Reduction

By Raoul Klingner[1,2], Jürgen Sell[1], Tanja Zimmermann[1], Andreas Herzog[2], Ulrich Vogt[2], Thomas Graule[2], Philipp Thurner[3], Felix Beckmann[4] and Bert Müller[5]

[1] Swiss Federal Laboratories for Materials Testing and Research, Wood-Department, Dübendorf, Switzerland
[2] Swiss Federal Laboratories for Materials Testing and Research, Department of High Performance Ceramics, Dübendorf, Switzerland
[3] Swiss Federal Laboratories for Materials Testing and Research, Department of Electronics and Metrology, Dübendorf, Switzerland
[4] Hamburger Synchrotronstrahlungslabor HASYLAB at Deutsches Elektronen-Synchrotron DESY, Hamburg, Germany
[5] Swiss Federal Institute of Technology, Computer Vision Laboratory, Zürich, Switzerland

Summary

The use of wood as a structure-giving material may be the key to producing temperature-resistant ceramics featuring high and directed porosity combined with necessary strength. The objective of this study was to develop a simple process to convert the evolutionarily optimized material wood into highly porous ceramics. Beech and pine, known to be relatively permeable, were pyrolyzed in a nitrogen atmosphere. The carbon-templates formed were infiltrated with various kinds of silica sol (SiO$_2$). The resulting SiO$_2$/C composite was transformed into a SiC-ceramic (silicon carbide) *via* carbothermal reduction. Through the described process the macroscopic pore-structure of wood was transformed exactly into SiC. The SiC-ceramic produced proved to be thermo-resistant. It remained stable in oxygen atmosphere at 1200 °C, after a SiO$_2$ coating around the SiC had been formed. This study focused on the alteration of the cell wall microstructure during the conversion of wood into SiC. Furthermore, the optimization of the individual process steps, pyrolysis, infiltration and ceramization along the most efficient route was pursued.

Introduction

In recent history nature has become more and more a model for innovation in structural design. Millions of years of evolution have produced structures perfectly adapted to the function they must fulfill and the stresses they must withstand. Relatively thin stems can reach heights up to 50 meters in positioning their heavy canopy into the light and still resist static and dynamic stresses like gravity or strong winds. At the same time they provide sufficient water-flow to the top of the tree without causing cell-collapse due to the pressure of the water column within the cells (Booker and Sell 1998). Form and structure of trees, therefore, are determined by the competing needs for optimizing strength and water transport (Niklas 1992). This results in structures that combine high strength and elasticity at very low weight.

In optimizing the design of technical components, the morphology of trees has already been successfully introduced as a model (Mattheck and Kubler 1995). The development of new methods to produce synthetic materials with improved properties based on biological materials and principles, often called biomimetics, also draws on wood. One way to make use of the unique structural design of wood in developing synthetic materials is by its ceramization (Byrne and Nagle 1997; Ota *et al.* 1995, 2000; Greil *et al.* 1998; Vogt *et al.* 2001; Shin *et al.* 2001).

During ceramization the morphology of wood is converted into a ceramic. The aim is to combine the porous and mechanically optimized structures of wood with superior material-properties of ceramic, like thermal, corrosive and abrasive resistance, to form a new material with a unique spectrum of qualities. The general process of engineering ceramics is based on creating a powder mixture that is shaped and sintered at high temperatures. Generally speaking, this procedure allows the manufacture of ceramics with isotropic porosity. If the orthotropic pore-structure of wood can be successfully converted into the ceramic state, a whole set of interesting applications for the new material seem possible, *e.g*, filtration of hot gases, catalyst carriers and other structural ceramics. Rapid prototyping of complex ceramic forms should be possible by easily shaping them in the wooden or pyrolyzed state and converting them afterwards.

Thus far, infiltration of the silicon donating source in the melted or gaseous phase has been favored for the conversion of wood into a SiC-ceramic (Greil *et al.* 1998; Herzog *et al.* 2000). Both routes prove to be difficult in manufacturing highly porous ceramics. The infiltration of melted silicon (1800 °C) forms a solid ceramic. To make use of the porosity of the material, free silicon has to be etched out in a further processing step. Infiltration of silicon in the gaseous phase forms a porous ceramic in a one-step process. But transformation to SiC is limited by template thickness, and consequently results in an incomplete conversion of samples thicker than 10 mm.

The objective of the experiments described in this paper was to develop a new process for the conversion of wood into a highly porous ceramic and to overcome aforementioned problems like size limitation and etching step.

Materials and Methods

In general, the samples of beech *(fagus sylvatica* L.*)* and pine *(pinus sylvestris* L.*)* had the dimensions 10 (axial) $\times$ 50 $\times$ 50 mm³. Alternatively, some experiments on pyrolysis and SiO_2-distribution after infiltration were done with 20 mm (axial) thick samples.

Pyrolysis

Pyrolysis was done in two steps. A low temperature furnace (Pyrotec 12h, Osnabrück, Germany) was used up to 800 °C. For further pyrolysis the furnace Carbolite CTF 16/75 818P (Sheffield, England) was available. Pyrolysis was carried out under nitrogen (99.995 Carbagas) atmosphere with flow-rates of 57 Nl/h, the heating ramp was 1 °C/min up to 500 °C and 5 °C/min up to the final temperature between 800 and 1400 °C.

Infiltration

After pyrolysis the carbon templates were evacuated in a desiccator, then the samples were flooded with silica sol for 30 min and finally kept under atmospheric pressure for 30 min. The silica sols Levasil 300 and Levasil 50 (Bayer, Leverkusen, Germany) were favored for the experiments (Table 1). After infiltration the samples were dried at 103 °C for 12 h and finally the mass increase due to the SiO_2 uptake was calculated.

Ceramization

After each infiltration, the Carbon/SiO_2 composite was ceramized at 1575 °C for 4 h with a heating ramp of 10 °C/min under argon (99.999 carbagas) atmosphere with flow-rates of 70 Nl/h. The infiltration-ceramization-cycle was repeated until the necessary weight percentage of SiO_2 for full conversion to SiC had been provided.

Equation [1] shows the need for 166 wt% SiO_2 (referring to the amount of carbon) in the sample for stoichiometric conversion of the provided amount of carbon to silicon carbide

Table 1. Characteristics of the silica sols

	Levasil 300	Levasil 50
Particle size	9 nm	50 nm
SiO_2-weight%	30 %	50 %
Stabilizing ion	NH_4^+	Na

Table 2. Reactions of ceramization *via* carbothermal reduction

$3C + SiO_2 \rightarrow SiC + 2CO$	[1]
$SiO_2 + C \rightarrow SiO + CO$	[2]
$SiO + 2C \rightarrow SiC + CO$	[3]
$SiC + 2SiO_2 \rightarrow 3SiO + CO$	[4]

(Table 2). The fully converted SiC sample was finally oxidized for 1 h at 1200 °C to burn off residual carbon and to form a protective SiO_2-coating.

Characterization

To visualize the different stages in the process of cell-wall conversion, a Scanning Electron Microscope with Field Emission Cathode was used (Jeol JSM 6300F, Tokyo, Japan). The pictures were taken with an acceleration voltage of 5 kV.

For measurements of the porosity of the samples in the different stages of conversion, a mercury porosimeter (PMI, Ithaca, USA) was used. Surface area was measured *via* nitrogen adsorption by the BET-method (PMI).

To visualize the internal SiO_2 distribution in dry samples after infiltration, Synchrotron Radiation based Micro-Computed Tomography (SRμCT) was performed (Beamline BW 2 at HASYLAB at DESY, Hamburg, Germany). At a photon energy of 13 keV and a spatial resolution of 3.5 μm (Müller *et al.* 2002a) 4 scans were necessary to scan the whole cylindrical shaped sample with a diameter of 2 mm and a height of 8 mm.

The phase composition of the fully converted samples was measured with X-ray diffraction (XRD Siemens D500, Munich, Germany).

Results and Discussion

Pyrolysis

During pyrolysis various changes in the cell-wall occur. At 400 °C most of the total weight loss of around 74 % has taken place as small molecules like H_2O and CO_2, along with complex aliphatic acids, carbonyl groups and alcohols, have emerged from the structure (Shafizahdeh and Chin 1977). They leave a very reactive lattice that, without melting of the polymer, immediately contracts and reorients as the short-chained molecules volatize (Byrne and Nagle 1997). The shrinkage caused is anisotropic. It is influenced by the macroscopic morphology of the wood, as well as the ultra-structure of the cell-wall. The transversal shrinkage is a combination of the pyrolysis behavior of the amorphous matrix (lignin and hemicellulose) and the embedded cellulose fibrils. The loss of the water between the single fibrils and the transition of the amorphous lignin into a carbon structure of denser order (Fig. 1 and 2) leads to more shrinkage in the transversal direction. Shrinkage in the axial direction is dominated by the cellulose chains. It is therefore reduced to the so-called cellulose molecule shrinkage. At pyrolysis temperatures from 800 °C to 1400 °C amorphous carbon was detected *via* XRD. Standard deviation in pore volume and infiltration measurements at pyrolysis at 800 °C and 1100 °C was higher than at 1400 °C. Changes in carbon modification along with
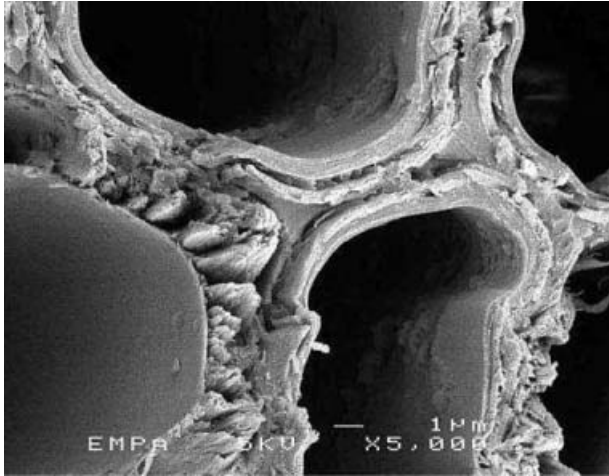
Fig. 1. Beech cell-wall, fracture surface, at the stage of 29 % weight loss in the course of pyrolysis.
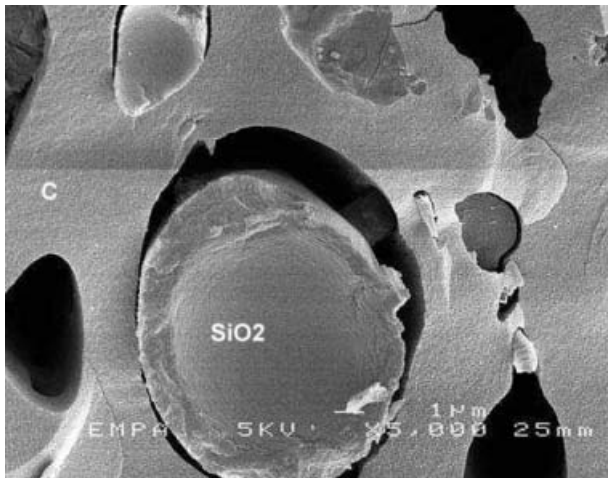

Fig. 2. Fracture surface of fully pyrolyzed beech after infiltration; SiO_2 in the cell lumina.

Table 3. Changes in the course of pyrolysis up to 1400 °C

		beech	pine
weight loss [%]	800 °C	73±0.4	73±0.2
	1400 °C	74±0.3	74±0.3
linear shrinkage [%]	Tangential	40±3.0	37±3.0
	Radial	30±2.0	31±2.0
	Axial	21±2.0	23±2.0
porosity [Vol. %]	Wood	56	69
	C-Template	65±4.0	74±4.0

the increase of pyrolysis temperature (Narciso-Romero and Rodriguez-Reioso 1999) may influence the wetting behavior of the template and could therefore be an explanation for this observation. Further increases in the pyrolysis temperature above 2000 °C result in graphite planes through longitudinal polymerization of the cellulose chains parallel to the former crystalline cellulose

(Tang and Bacon 1964). For process optimization a pyrolysis temperature of 1400 °C seems most suitable. Despite the macroscopical shrinkage, the pore-volume of the pyrolyzed sample increases (Table 3).

Infiltration

After pyrolysis, the exact replica of the former macroscopic wood structure remains (Fig. 2). The porous structure consists only of carbon that will be the reaction partner of silicon oxide in the further processing to silicon carbide (Equation [1]–[3]). In the next step, the silicon source, in this experiment silica sol (SiO_2), must be brought into close contact with the carbon to enable the ceramization reaction. Here the silica sol is infiltrated at room temperature. Therefore, no instant reaction occurs, as with liquid or gaseous silicon at high temperature (>1600 °C). This simplifies the process as the actual ceramization is carried out in a separate high temperature step under controlled conditions.

To introduce the silica sol into the carbon-template, the infiltration process can be carried out in different ways. Either infiltration is repeated several times (repeated infiltration) until enough SiO_2 for full conversion (166 wt%) is incorporated into the sample and then total conversion follows in a single ceramization step. Or, in a cyclic process each infiltration step is followed by a ceramization (cyclic infiltration) until the sample is fully converted. The latter process showed an increased amount of SiO_2 absorbed per infiltration step (Fig. 3).

Depending on the sol used, it takes several infiltration-ceramization-cycles to provide the necessary amount of SiO_2 in the carbon-template. Using Levasil
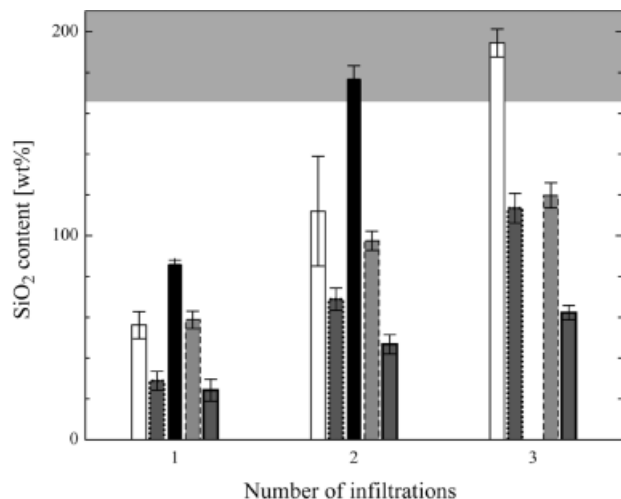

Fig. 3. Number of infiltrations compared with measured weight increase of the sample after drying. Pine and beech were infiltrated with different sols (Table 1) and processes. White bar: Pine, 30 %, cyclic infiltration. Grey bar, dotted line: Beech, 30 %, cyclic infiltration. Black bar: Beech, 50 %, cyclic infiltration. Light grey bar, dashed line: Pine, 30 %, repeated infiltration. Grey bar, thick line: Beech, 30 %, repeated infiltration. SiO_2 demanded for total conversion (166 wt%) is shaded in grey.

50 and beech, after two cycles the sufficient amount of SiO$_2$ (166 wt%) for stoichiometric conversion is infiltrated (Fig. 3).

Hg-porosimetry and SRµCT demonstrate a sufficient and homogenous presence of SiO$_2$ throughout the sample. SRµCT yields a 3-D mapping of the X-ray linear absorption coefficient across the sample. With Si and C differing sufficiently in X-ray absorption, it is possible to separate both phases in the retrieved tomograms. This allows the separation of carbon and SiO$_2$ (Fig. 4) and the extraction of the SiO$_2$ distribution as a function of sample depth, as shown in Figure 5. The four curves were retrieved from the scans. The thresholds, set in each tomogram in order to suppress all elements without SiO$_2$, are

Fig. 6. Hg-porosimetry depicting pore-size distribution through the relation of certain pore diameters and their frequency of appearance in the given volume. Beech C-template (●), infiltrated beech C-template (○).

found by histogram analysis (Müller *et al.* 2002b). The differences in the overlapping regions in Figure 5 are most probably attributed to locally varying presence of higher harmonics of the selected X-ray wavelength during data acquisition.

For beech, after infiltration and drying most of the vessels are completely filled with SiO$_2$. (Fig. 4 and 6). Measured porosity around 0.8 µm and 8 µm appear to be gaps and cracks due to shrinkage of the SiO$_2$ in the process of drying and agglomeration (see also Fig. 2).

Fig. 4. 3-D SRµCT-picture of a cylindrical sample of pyrolyzed beech after infiltration with ~2 mm diameter and ~8 mm height. A: SiO$_2$/C composite, phases not separated. At the bottom of the sample residual glue of the fixation in the tomograph is visible. B: Only the separated Si-phase is depicted showing SiO$_2$ columns of infiltrated vessels throughout the whole sample. This shows a sufficient infiltration on SiO$_2$ *via* the vessels of beech. Columns are separated in shorter sections due to shrinkage of the silica sol during drying.
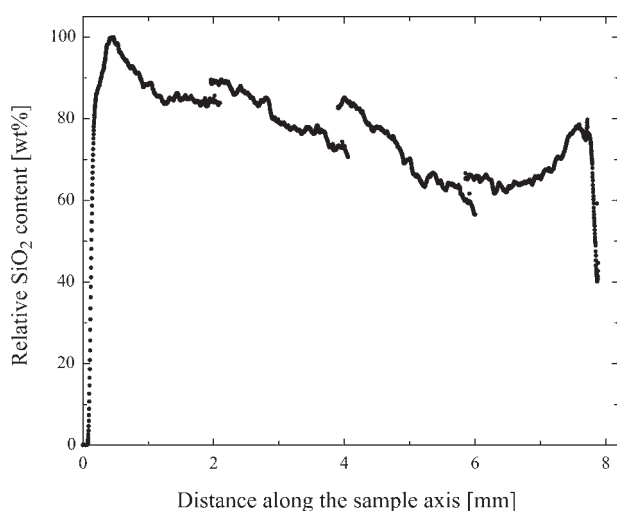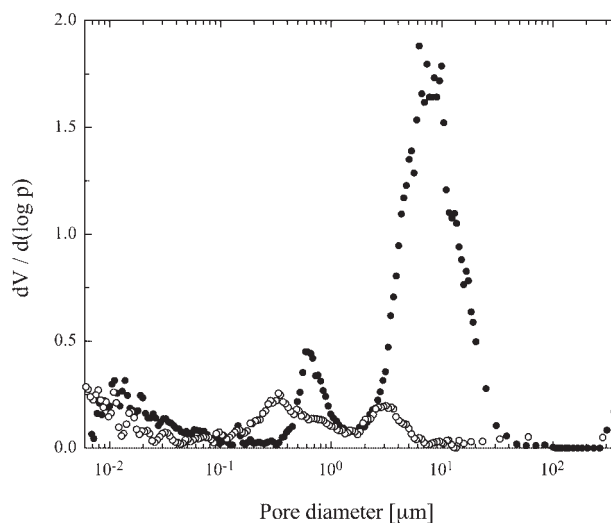
Ceramization

The principle reaction of a metal oxide and a carbon source as the given wood-derived carbon-template is called carbothermal reaction. Carbon is the cause of reduction and is itself partly oxidized to CO (Equation [2]). The formation of SiC is not a solid state reaction but dominated by the gas-phase SiO originating from reduced SiO$_2$ as seen in Equation [3]. Besides the modifications of the carbon source, the partial pressure of the SiO and the CO is of decisive significance in the reaction. Within the temperatures 927 °C and <1727 °C SiO is the dominating gas. Above 1027 °C CO as a reaction product limits the conversion and must be removed (Weimer 1997). The Gibb's free enthalpy (ΔG) is zero at a temperature of 1515 °C, at higher temperatures the balance of the reaction [1] moves towards the synthesis of the reaction products SiC and CO as the free reaction enthalpy becomes negative.

Fig. 5. Extraction of the SiO$_2$ distribution as a function of sample depth demonstrating a relatively homogeneous distribution of SiO$_2$ across the sample axis.

The dominance of the gas-phase SiO explains the full conversion of the sample to SiC even though inhomogeneous SiO$_2$-distribution is observed as some pores are not filled with SiO$_2$. Compared to the vessels of beech, its fibers in the center of the sample, which are not cut at the ends, show little permeability (Wardrop and Davies
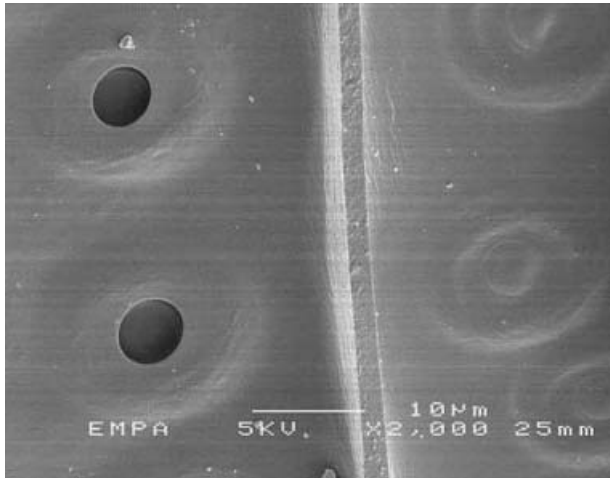
Fig. 7. Radial fracture surface of a carbon-template of pine with aspirated bordered tips.
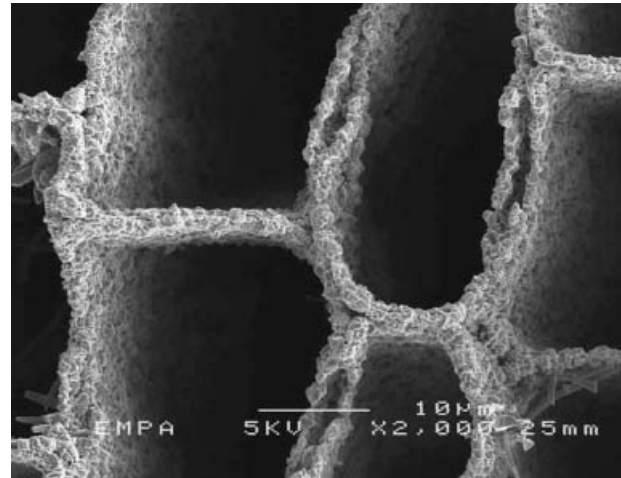

Fig. 9. Fracture surface of fully converted earlywood pine tracheids with bordered pits.
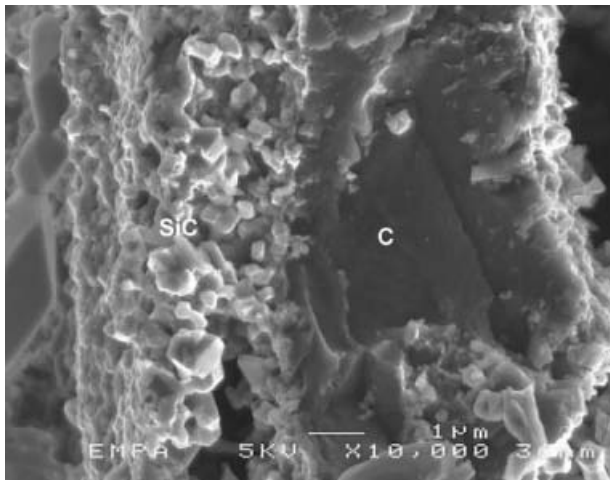

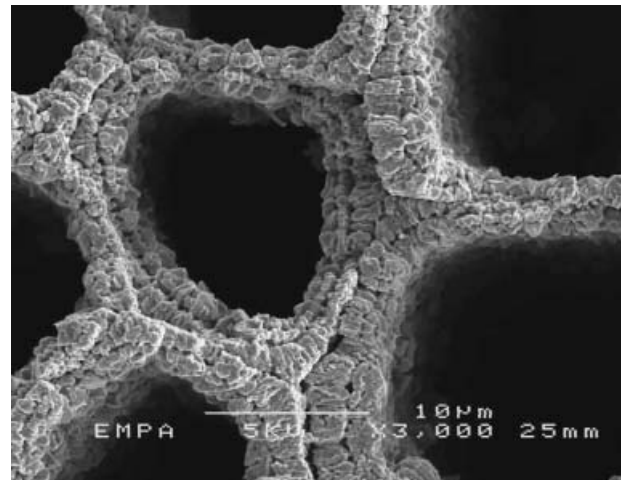**Fig. 8.** Primary stage of SiC-growth through the pyrolyzed cell wall.

Fig. 10. Fracture surface of ceramized pine latewood with unique crystal orientation.

1961). Tip aspiration as the main reason for low permeability in pine (Siau 1971) is sometimes observed in the pyrolyzed state (Fig. 7). This results in a lower SiO_2-concentration in the core of the pine sample.

At rather high levels of SiO_2-concentration, full reaction with the carbon present does not occur. Some SiO leaves the sample without reaction, decreasing reaction efficiency. Therefore, the homogeneous distribution of SiO_2 and consequently a constant SiO release rate within the sample is key for successful conversion. Cyclic change of infiltration and ceramization seems to provide the best results concerning the quality of conversion and the stability of the sample during handling, yet no elastomechanical experiments were performed to quantify this assumption.

The primary growth of SiC occurs through direct contact of the SiO with the carbonized cell-wall surface (C). Further growth towards the former compound middle lamella is controlled by diffusion of SiO through the primary SiC-layer and therefore depends on SiC layer

thickness and density. Figure 8 shows SiC formation between longitudinal tissue and ray parenchyma, which is difficult to infiltrate. Evidently SiC formation proceeds from well-infiltrated regions with higher SiO pressure towards poorly infiltrated cells. In Figure 8 SiO pressure could only facilitate ceramization of parts of the cell wall. Another cycle of infiltration and ceramization would be necessary for total conversion. With the appropriate amount of SiO_2 and sufficient time, the cell walls of the whole sample are fully converted to SiC. A surplus of SiO_2 in an area of converted cell walls can also lead to a destruction of the formed SiC, [equation 4].

With the described process pine and beech were successfully transformed into a silicon carbide ceramic (Figs. 9–12). The converted cell walls have a granular appearance with a crystal size up to 1 µm. The ceramized pine cell wall is remarkable in the orientation of SiC-crystals along the former middle lamella. The reason for this orientation is not yet clear. It is neither
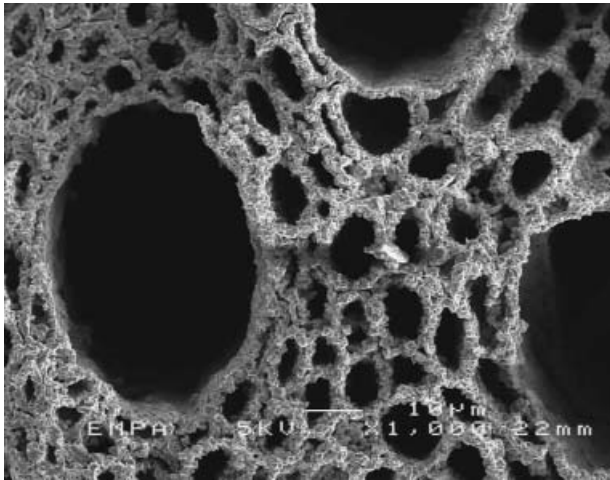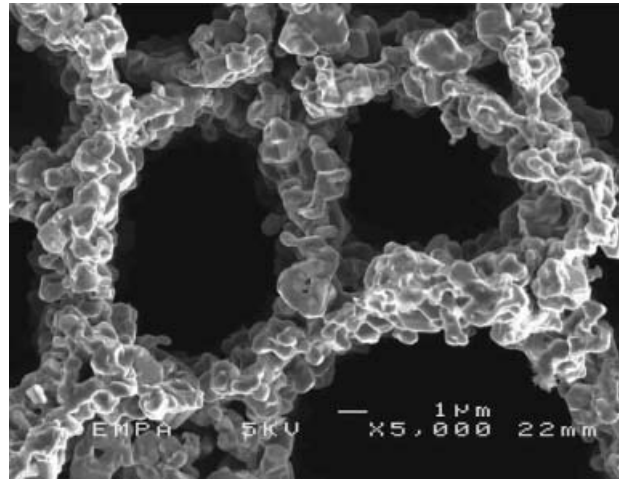
Fig. 11. Ceramized beech.

Fig. 12. Ceramized beech fibers in detail.

found in the carbon state of pine nor in any of the beech samples during conversion.

Besides SEM, the total conversion into SiC was also demonstrated through XRD-scans. The XRD spectrum in Figure 13 shows clear SiC peaks suggesting full conversion. After cyclic oxidation the wood derived SiC-ceramics show a distinct SiO_2-glas peak next to SiC peaks (Fig. 13). Like other non-oxide ceramics, the wood derived SiC is not stable against oxidation in the beginning. In oxidation tests at 1200 °C for 64 h in air, the ceramics show the typical parabolic weight increase due to the forming of SiO_2 around the SiC-crystals (Fig. 14). For SiC-wood an oxidation constant of 3×10^{-14} kg/m^{4}s was calculated according to

$$(\Delta m/A_0)^2 = k_p t \qquad [5]$$

Surface area of SiC-wood was determined by BET as 1.5 m^2/g. The oxidation constant k_p of wood-derived ceramics shows improvement in oxidation behavior compared to the oxidation behavior of SiC powders as Kriegesmann (1996) calculated a constant of 2.6×10^{-11} kg/m^{4}s for SiC powder sized between 20–41μm.

The SiO_2-layer around the SiC-crystals passivates the surface for further oxidation. In SEM-pictures the SiO_2-layer around the SiC-crystals can be seen as a clear smoothing of the cell-wall structure as compared to non-oxidized samples (Fig. 15).

Conclusion

Wood offers a wide variety of evolutionarily optimized structures for other fields of material science such as ceramics. With the described method of the ceramization of wood *via* the infiltration of silica sol, highly porous ceramics can be produced. In the process of converting the cell-wall material into SiC the original pore-structure of the wood remains constant. Wood-derived ceramics combine high and oriented porosity with structural integrity. The porous ceramics produced basically
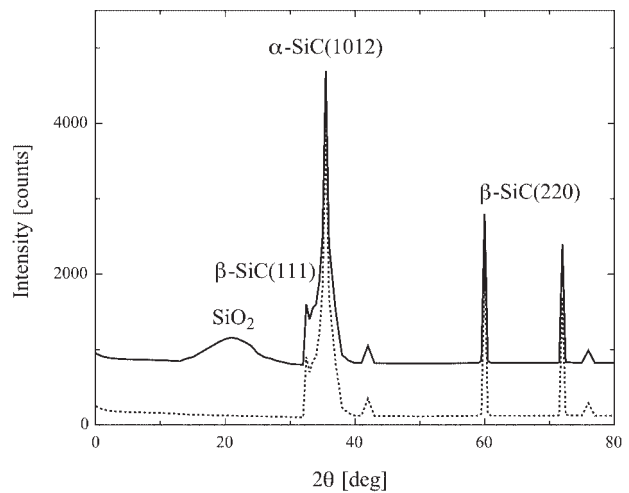

Fig. 13. XRD-scans of wood derived ceramics fully converted to SiC ($\cdots$) and after oxidation with an additional peak of SiO_2 in the scan (—).
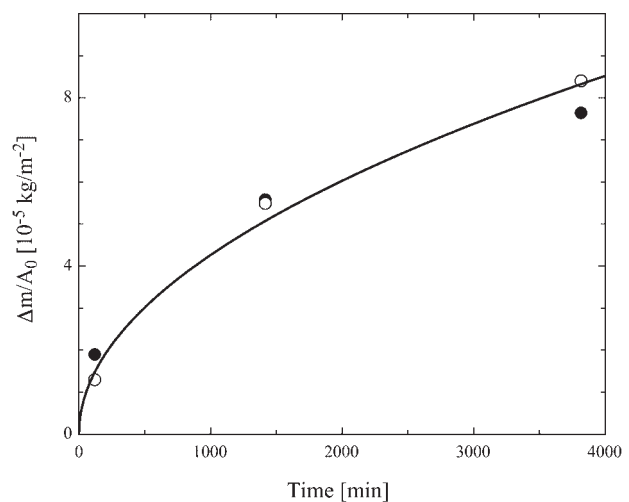

Fig. 14. Weight increase through oxygen-intake during oxidation and parabolic curve fit according to Equation [5]. Beech (●), pine (○) and $\Delta m/A_0 \sim t^{1/2}$ (—).
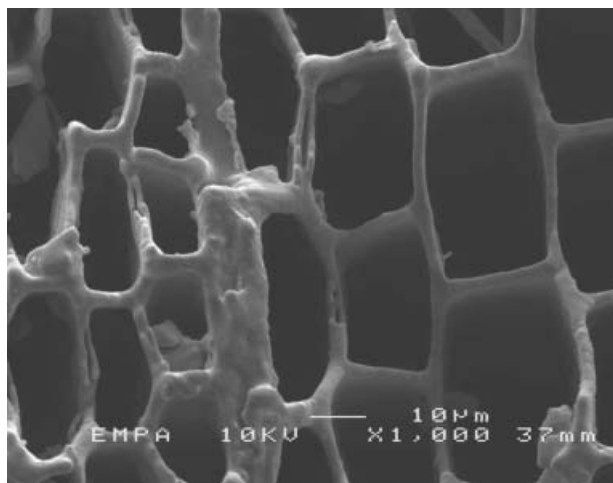
Fig. 15. Fracture surface of oxidized (64 h at 1200 °C in air) SiC-ceramic derived from pine. Compared to non-oxidized pine in Figure 12, here the SiO_2-glass cover around the crystals can be clearly seen.

fulfil the needs for technical use, although further research concerning porosity, strength and consistency of the material needs to be done, before this seems feasible. The developed process is applicable to engineered wood products (*e.g.*, particle board), cardboard or filter papers as well. Compared to untreated wood this would result in more homogeneous ceramics.

Acknowledgements

References

Booker, R. and J. Sell. 1998. The nano-structure of the cell wall of softwoods and its function in a living tree. Holz Roh-Werkstoff *56*, 1–8.

Byrne, C.E. and D.C. Nagle. 1997. Carbonization of wood for advanced material applications. Carbon *35*, 259–266.

Greil, P., T. Lifka and A. Kaindl. 1998. Biomorphic silicon carbide from wood. I: Processing and microstructure. II: Mechanical properties. J. Europ. Ceram. Soc. *18*, 1961–1975.

Herzog, A., U. Vogt, T. Graule, T. Zimmermann and J. Sell. 2000. Characterization of the pore structure of biomorphic cellular silicon carbide derived from wood by mercury porosimetry. *In:* Ceramic Materials and Components for Engines. Eds. J.G. Heinrich, F. Aldinger. Wiley, Weinheim. pp. 505–511.

Kriegesmann, J. 1996. Technische Keramische Werkstoffe. Siliciumcarbid-Keramik. Deutscher Wirtschaftsdienst, Köln. Chap. 5.4.1.1, p. 20. [German only].

Müller, B., P. Thurner, F. Beckmann, T. Weitkamp, C. Rau, R. Bernhardt, E. Karamuk, L. Eckert, S. Buchloh, E. Wintermantel, D. Scharnweber and H. Worch. 2002a. Three-dimensional evaluation of biocompatible materials by micro-tomography using synchrotron radiation. *In:* Proceedings of SPIE 4503. pp. 178–188.

Müller, B., F. Beckmann, M. Huser,. F.A. Maspero, G. Szekely, K. Ruffieux, P. Thurner and E. Wintermantel. 2002b. Non-destructive three-dimensional evaluation of a polymer sponge by micro-tomography using synchrotron radiation. Biomolecular Engineering *19*, 73–78.

Mattheck, C. and H. Kubler. 1995. Wood – The Internal Optimization of Trees. Springer, Berlin. pp. 27–37.

Narciso-Romero, F.J. and F. Rodriguez-Reioso. 1999. Influence of carbon material on the synthesis of silicon carbide. Carbon *37*, 1771–1778.

Niklas, K.J. 1992. Plant Biomechanics. Chicago Univ. Press, Chicago. pp. 20–32.

Ota, T., M. Takahashi, T. Hibi, M. Ozawa, S. Suzuki and Y. Hikichi. 1995. Biomimetic process for producing SiC "wood". J. Am. Ceram. Soc. *78*, 3409–3411.

Ota, T., M. Imaeda, H. Takase, M. Kobayashi, N. Kimoshita, T. Hirashita, H. Miyazaki and Y. Hikichi. 2000. Porous titania ceramic prepared by mimicking silicified wood. J. Am. Ceram. Soc. *83*, 1521–1523.

Shafizadeh, F. and P. Chin. 1977. Thermal deterioration of wood. *In:* Wood Technology. Chemical Aspects. ACD Symposium series, Am. Chem. Soc., Washington D.C. pp. 55–81.

Shin, Y., J. Liu, J.H. Chang, Z. Nie and G. Exarhos. 2001. Hierarchically ordered ceramics through surfactant-templated sol-gel mineralization of biological cellular structures. Adv. Materials *13*, 728–731.

Siau, J.F. 1971. Flow in Wood. Syracuse University Press, New York. pp. 17–34.

Tang, M. and R. Bacon. 1964. Carbonization of cellulose fibers – I. Low temperature pyrolysis. Carbon *2*, 211–220.

Vogt, U., A. Herzog, T. Graule, R. Klingner, T. Zimmermann and O. Paris. 2001. Wood derived SiC ceramics with oriented porous structures *via* carbothermal reduction, *In:* Proceedings of HTCMC IV in High Temperature Ceramic Matrix Composites. Eds. W. Krenkel, R. Naslain, H. Schneider. Wiley, Weinheim. pp. 420–425.

Wardrop, A.B. and G.W. Davies. 1961. Morphological factors relating to the penetration of liquids into wood. Holzforschung *15*, 129–141.

Weimer, A.W. 1997. Carbide, Nitride and Boride Materials Synthesis and Processing. Chapman and Hall, Cambridge. pp. 94–97.

Raoul Klingner[1]
Jürgen Sell
Tanja Zimmermann
Andreas Herzog
Ulrich Vogt
Thomas Graule
Philipp Thurner
Swiss Federal Laboratories for Materials Testing and Research
CH-8600 Dübendorf
Switzerland

Felix Beckmann
Hamburger Synchrotronstrahlungslabor HASYLAB at
Deutsches Elektronen-Synchrotron DESY
D-22603 Hamburg
Germany

Bert Müller
Swiss Federal Institute of Technology
Computer Vision Laboratory
CH-8092 Zürich
Switzerland

---

[1] Corresponding author